Interaction of Myosin Subfragment 1 with Forms of Monomeric Actin †

ARTICLE *in* BIOCHEMISTRY · APRIL 2003

Impact Factor: 3.02 · DOI: 10.1021/bi020597q · Source: PubMed

4 AUTHORS, INCLUDING:

Dietmar J Manstein
Hannover Medical School
148 PUBLICATIONS **4,566** CITATIONS
SEE PROFILE

Hans Georg Mannherz
Ruhr-Universität Bochum
118 PUBLICATIONS **2,719** CITATIONS
SEE PROFILE

Interaction of Myosin Subfragment 1 with Forms of Monomeric Actin[†]

Edda Ballweber,[‡] Peter Kiessling,[‡,§] Dietmar Manstein,[||] and Hans Georg Mannherz*[,‡]

Department of Anatomy and Embryology, Ruhr-University, Bochum, Germany, and Max-Planck-Institute for Medical Research, Heidelberg, Germany

Received September 24, 2002; Revised Manuscript Received January 3, 2003

ABSTRACT: The ability of myosin subfragment 1 to interact with monomeric actin complexed to sequestering proteins was tested by a number of different techniques such as affinity absorption, chemical cross-linking, fluorescence titration, and competition procedures. For affinity absorption, actin was attached to agarose immobilized DNase I. Both chymotryptic subfragment 1 isoforms (S1A1 and S1A2) were retained by this affinity matrix. Fluorescence titration employing pyrenyl-actin in complex with deoxyribonuclease I (DNase I) or thymosin β_4 demonstrated S1 binding to these actin complexes. A K_D of 5×10^{-8} M for S1A1 binding to the actin−DNase I complex was determined. Fluorescence titration did not indicate binding of S1 to actin in complex with gelsolin segment 1 (G1) or vitamin D-binding protein (DBP). However, fluorescence competition experiments and analysis of tryptic cleavage patterns of S1 indicated its interaction with actin in complex with DBP or G1. Formation of the ternary DNase I−acto−S1 complex was directly demonstrated by sucrose density sedimentation. S1 binding to G-actin was found to be sensitive to ATP and an increase in ionic strength. Actin fixed in its monomeric state by DNase I was unable to significantly stimulate the Mg^{2+}-dependent S1-ATPase activity. Both wild-type and a mutant of *Dictyostelium discoideum* myosin II subfragment 1 containing 12 additional lysine residues within an insertion of 20 residues into loop 2 (K12/20−Q532E) were found to also interact with actin−DNase I complex. Binding of the K12/20−Q532E mutant to the actin−DNase I complex occurred with higher affinity than wild-type S1 and was less sensitive to mono- and divalent cations.

The contractile protein actin can exist in two different forms of macromolecular organization: the monomeric or G-actin at low ionic strength and the filamentous or F-actin in the presence of high salt or divalent cations in the millimolar range. It was originally observed by Straub (*1*) that only F-actin is able to form active complexes with myosin and to activate its Mg^{2+}-dependent ATPase activity. Therefore, it has been supposed that the binding site for myosin or its proteolytic fragment subfragment 1 (S1) on F-actin is formed by adjacent monomers of the actin filament. Indeed, image reconstruction data of electron microscopic pictures of S1 decorated F-actin have indicated the simultaneous binding of one S1 molecule to two adjacent actin monomers along the long-pitch helix (*2*, *3*, for a review see ref *4*). Alternatively, it has been suggested that actin undergoes a structural change during polymerization, rendering it able to interact with myosin heads (*5*, *6*). Both models imply that G-actin at low salt is in a conformation not able or to only weakly interact with myosin. However, myosin and its fragments (like heavy meromyosin or S1) are able to induce polymerization of G-actin (*7*−*10*). To inhibit myosin subfragment 1 induced polymerization of actin and to study its interaction with G-actin, we used stoichiometric 1:1 complexes of actin with deoxyribonuclease I (DNase I), gelsolin segment 1 (G1), thymosin β_4 (Tβ_4), or vitamin D-binding protein (DBP). In these complexes, actin is fixed in monomeric state and cannot form high molecular aggregates even in the presence of high salt or divalent cations (*11*−*16*). In addition, the atomic structures of these complexes have been solved (*17*−*21*); therefore, it was regarded as possible to delimit the actin binding sites for subfragment 1.

Chemical cross-linking experiments have indicated that the main contact area of S1 heavy chain is located on subdomain 1 of actin (*22*, *23*) and the light chain A1 to the C-terminal region of actin (subdomain 1) (*22*). Image reconstruction of electron microscopic pictures of negatively stained S1 decorated F-actin have supported these data and given further insight into the molecular details of the actin−S1 interface at rigor conditions (for reviews see refs *4* and *24*). S1 binding to actin is believed to occur in a number of discrete steps. Initially, a collision complex stabilized by ionic

[†] This work was financially supported by the Deutsche Forschungsgemeinschaft, Bonn, Germany (Ma 807/14-1).

* Corresponding author. Dr. H. G. Mannherz, Abteilung für Anatomie und Zellbiologie, Ruhr-Universität Bochum, Universitätsstr. 150, D-44780 Bochum, Germany. Tel.: +49-234-3224553; Fax: +49-234-3214474; E-mail: hans.mannherz@ruhr-uni-bochum.de.

[‡] Ruhr-University.

[||] Max-Planck-Institute for Medical Research.

[§] Present address: Aventis Behring, P.O. Box 1230, D-35002 Marburg, Germany.

[1] Abbreviations: ATP, adenosine triphosphate; ADP, adenosine diphosphate; DNase I, deoxyribonuclease I (EC 3.1.21.1.); DBP, vitamin D binding protein; EGTA, ethylene-glycol-bis-(β-aminoethylether); EDC, 1-ethyl-[3-(dimethylamino)-propyl]-carbodiimide; G1, gelsolin segment 1; Hepes, *N*-2-hydroxyethylpiperazine-*N*′-2-ethansulfonic acid; mant-ATP, 3′-*O*-(*N*-methylanthranidoyl)-adenosine 5′-triphosphate; MES, 2-(*N*-morpholino)ethanesulfonic acid; S1, myosin subfragment 1; S1A1, S1 containing the M_r 21 000 light chain; S1A2, S1 containing the M_r 17 000 light chain; Tβ_4, thymosin β_4.

10.1021/bi020597q CCC: $25.00
Published on Web 02/20/2003

interactions is formed. This step is believed to involve the negatively charged N-terminus of actin and the lysine rich loop 2 of S1 spanning residues Tyr626 to Gln647 (numbering from chicken skeletal myosin; see also ref *4*). It is assumed that this initial complex is further stabilized by the so-called cardiomyopathy loop of S1 (residues Pro404 to Lys415) and hydrophobic contacts involving a helix−loop−helix motif (Pro529 to His558). This latter contact is supposed to form the main stereospecific contact area leading to strong binding between S1 and actin (*25*). These contacts are established between S1 and one single actin monomer (for review see ref *4*). Finally, a fourth contact is formed between S1 and the actin monomer below along the long-pitch helix by the so-called secondary actin binding site of S1 (residues Lys567 to His578; for reviews see refs *4* and *24*).

Assuming that actin-sequestering proteins such as DNase I, gelsolin segment 1, DBP, and thymosin β_4 do not completely cover the myosin binding sites on actin, we studied the interaction of S1 and actin in complex with these binding proteins. Previously, the formation of a ternary complex of actin, DNase I, and S1 has been suggested from inhibition studies of internally cross-linked G-actin (*26*−*28*) and the ability of native or chemically cross-linked G-actin−S1 complex to inhibit the DNA degrading activity of DNase I (*29*, *30*). Using pyrenyl-actin, the binding constant of S1 to actin in the presence of DNase I was determined and found to be decreased by a factor of about 100 in comparison to F-actin (*27*, *29*). Here we report experiments extending these studies including a number of additional actin sequestering proteins able to fix actin in monomeric form and wild-type and mutant S1s from *Dictyostelium discoideum* myosin II (*31*, *32*).

MATERIALS AND METHODS

Protein Preparations. Actin was isolated from acetone dried powder obtained from rabbit psoas and back muscle (*33*) and further purified according to ref *34*. Pyrene-labeled actin (pyrenyl-actin) was prepared exactly as detailed by Koujama et al. (*35*). Chymotryptic S1 from rabbit psoas muscle myosin was prepared and separated into S1A1 and S1A2 isoforms (*36*). SDS−PAGE indicated that subfragment 1 containing the light chain A1 (S1A1) was almost 100% pure, whereas subfragment 1 with the light chain A2 (S1A2) often still contained an additional trace of the light chain A1. Wild-type S1 terminating after residue 761 and the mutant of Dictyostelium myosin II containing an additional insert of 20 amino acids within loop 2, 12 of which are lysine residues, and a Q532E point mutation were expressed in *D. discoideum* (*31*).

Bovine pancreatic DNase I was a commercial product from Paesel & Lorei (Frankfurt, Germany) and further purified by chromatography on hydroxylapatite (*37*). The N-terminal domain of plasmatic gelsolin (segment 1) was expressed in *Escherichia coli* and purified as described (*15*). Thymosin β_4 was isolated from bovine spleen (*38*) and generously provided by Prof. Hannappel and Dr. Huff (Erlangen, Germany). DBP was purified from outdated human plasma (*39*). Actin was ADP-ribosylated by Clostidrium perfringens iota-toxin (*40*). Iota toxin was kindly provided by Prof. K. Aktories (Freiburg, Germany). Actin in complex with these binding proteins was usually extensively dialyzed to remove free ATP. Alternatively, it was treated with 10% (v/v) Dowex 1X8 for one minute on ice immediately before use.

Analytical Procedures. Actin concentration was determined spectrophotometrically at 290 nm using an absorption coefficient of 0.63 mg mL^{-1} cm^{-1} (*41*). Concentrations of other proteins were determined by using the Bradford procedure (*42*). Polyacrylamide gel electrophoresis in the presence of sodium dodecyl sulfate (SDS−PAGE) was performed according to Laemmli (*43*). Immunoblots were performed as described previously (*44*) using a monoclonal anti-sarcomeric actin and a polyclonal anti-subfragment 1 antibody at dilutions of 1:5000 and 1:10000, respectively. Retained antibodies were visualized by using a secondary biotinylated sheep anti-mouse IgG followed by a streptavidin−biotinylated horseradish peroxidase (HRP) complex or by employing a goat anti-rabbit IgG-HRP-peroxidase complex (*44*).

Limited tryptic digestion of S1 was performed at a trypsin-to-substrate ratio of 1:100 (w:w) according to ref *5*. Cleavage patterns were analyzed for S1 on its own and after mixing with F-actin or G-actin in complex with DNase I, DBP, or G1 at a 1:1 molar ratio. The tryptic patterns were followed in time course experiments, subjecting an aliquot at a given time to 10−18% gradient SDS−PAGE to analyze the generation of S1 fragments.

Density-gradient (zonal rate) centrifugation of the ternary complex of actin−DNase I−S1 was performed using a sucrose gradient from 10 to 40% in a SW 41 rotor (Beckman) at 163000*g* for 72 h and 4°C (*45*). Twelve samples of 1 mL were fractionated and analyzed by monitoring the protein concentration at 290 nm or the Bradford procedure (*42*) and by SDS−PAGE.

Steady-state rates for the Mg^{2+}-dependent ATPase of S1 were determined using a linked enzyme assay (*46*). DNase I activity was determined by measuring the increase in absorbance at 260 nm (hyperchromicity test) (*37*, *47*) using a Beckman spectrophotometer DU 640.

Affinity Chromatography. For affinity binding studies, divinylsulfone agarose (Mini-Leak) was used as an affinity matrix to immobilize DNase I. Usually 20 mg of DNase I was coupled to 3 mg of affinity matrix according to the manufacturer's protocol and packed in a column (10 × 1 cm). G-actin at an equimolar ratio was allowed to bind to DNase I in G-buffer (5 mM Hepes-OH, pH 7.4, 0.1 mM $CaCl_2$, 0.5 mM NaN_3, 0.2 mM ATP). Before loading, the column was washed by 100 mL G-buffer supplemented with 1 M NaCl followed by 100 mL of G-buffer plus 5 mM ATP and then equilibrated with the appropriate running buffer without ATP (buffer A: 2 mM Tris-HCl, pH 8.0, 0.2 mM $CaCl_2$, 2 mM $MgCl_2$, 0.1 mM NaN_3). The elution profile was monitored spectrophotometrically at 290 nm or by using the Bradford procedure (*42*) and by analysis of aliquots on SDS−PAGE. Usually 20 fractions of 1 mL each were collected.

To exclude denaturation of the DNase I immobilized actin before and after the binding and release steps of subfragment 1, we analyzed its nucleotide binding capacity using ^{3}H-ATP. To this aim, DNase I immobilized actin was incubated with 0.05 mM ATP supplemented with ^{3}H-ATP for 1 h at room temperature, washed first with G-buffer, and then with G-buffer supplemented with 1 mM EDTA to release actin bound nucleotide. The eluted radioactivity of 1 mL fractions

was determined by liquid scintillation counting. We did not observe a significant decrease of the ^{3}H-ATP binding capacity after the S1 binding and release steps.

Fluorescence Titration Experiments. Fluorescence measurements employing pyrene-labeled actin were performed using a Shimadzu RF 5001PC spectrofluorometer with wavelength settings of 365 and 385 nm for excitation and emission, respectively. Increasing concentrations of S1A1 were added to free pyrenyl-G-, -F-, or -ADP-ribosylated-G-actin and pyrenyl-G-actin in complex with DNase I, thymosin β_4, gelsolin segment 1, or DBP. For these experiments, the proteins were taken up in G-buffer. The relative fluorescence was read immediately after S1A1 was applied to the samples. To determine the affinity constants, the fluorescence intensity was plotted versus the S1A1 concentration. Theoretical binding curves for 1:1 complexes containing monomeric actin and S1A1 were calculated (EXCEL program) to determine K_D values (*44*) using mass equations given in ref *48* to calculate the binding curves for affinity determination.

Competition Experiments. The binding and affinity of S1A1 to unlabeled actin on its own or in complex with binding proteins was also determined by competitive binding of pyrenyl-F-actin and unlabeled actin to S1A1 (*48*). To this end, pyrenyl-F-actin stabilized by equimolar phalloidin was decorated with S1A1. Then increasing concentrations of the competitor were added. As competitor unlabeled F-actin (positive control), G-actin, G-actin−DNase I- and actin−G1 complex were tested. Titration series with unlabeled F-actin and actin−DNase I complex contained 2 mM $MgCl_2$ in G-buffer (F-buffer) to establish actin polymerizing conditions. In titration assays with free G-actin, actin−DNase I and actin−G1 complex the $MgCl_2$ was omitted. The fluorescence intensity was recorded immediately after the addition of S1A1. The excitation and emission wavelengths were set at 365 and 385 nm, respectively. The affinity was determined by plotting the fluorescence intensity versus the concentration of the competitor. Theoretical competition binding curves based on a K_D value of 0.5 nM for S1A1 binding to pyrenylated F-actin (*48*) were calculated to determine the K_D values of S1A1 to unlabeled monomeric actin in complex with sequestering proteins.

Determination of mant-ADP Dissociation from S1. Nucleotide displacement from subfragment 1 by actin was determined by using mant-ATP (3′-*O*-(*N*-methylanthranidoyl)-adenosine 5′-triphosphate). S1 was mixed with a substoichiometric amount of mant-ATP and incubated to allow complete hydrolysis to mant-ADP and release of inorganic phosphate (P_i) (*49*). Binding of mant-nucleotide to S1 results in a fluorescence increase that was determined with wavelength settings at 356 and 445 nm for excitation and emission, respectively. After addition of F-actin or actin−DNase I to mant-ADP−S1 the release of mant-ADP was determined by the fluorescence decrease.

Cross-Linking Experiments. Complexes of S1 with actin−DNase I complex (generated by mixing G-actin and DNase I at a molar ratio of 1:2) were obtained by mixing actins and S1 at equimolar ratio. Cross-linking reactions between S1 and actin of the actin−DNase I complex were performed similar to ref *5* using 0.55 mM EDC (1-ethyl-[3-(dimethylamino)-propyl]carbodiimide) final concentration in 55 mM MES-buffer (*N*-morpholinoethanesulfonic-acid), pH 6.0, and allowed to proceed for 1 h at room temperature.

Materials. EDC was a product of Pierce (Rotterdam, The Netherlands). MINI-LEAK was purchased from Kem-EN-Tec (Copenhagen, Denmark). Affi-Gel 15 was a product of Pharmacia (Freiburg, Germany). ^{3}H-ATP was a product of Amersham Buchler (Braunschweig, Germany). Nucleotides were purchased from Pharma Waldhof (Düsseldorf, Germany). Hepes was a product of Carl Roth (Karlsruhe, Germany). The monoclonal anti-sarcomeric actin antibody was a commercial product of Sigma (clone 5C5; München, Germany). The secondary anti-mouse IgG and the -rabbit IgG were obtained from Amersham (Braunschweig, Germany) and BioRad (München, Germany), respectively. 3′-*O*-(*N*-methylanthranidoyl)-adenosine 5′-triphosphate (mant-ATP) was a generous gift of Prof. R. S. Goody (Dortmund, Germany). All other reagents were of analytical grade.

RESULTS

Affinity Adsorption of Subfragment 1 to Immobilized Actin−DNase I Complex. For affinity absorption, purified DNase I was immobilized to divinyl sulfone activated agarose. Thus immobilized DNase I was loaded with G-actin and extensively washed before applying 1 mg of S1. The column was subsequently washed with 20 mL of buffer A, followed by 20 mL buffer A plus a given concentration of ATP. Fractions of 1 mL were collected and analyzed for protein by the Bradford procedure and SDS−PAGE. The results shown in Figure 1 indicate that the S1 applied was completely retained by immobilized actin−DNase I complex, but eluted when supplementing buffer A with ATP. Elution of retained S1 started at about 10 μM ATP and was complete at 2 mM. Both chymotryptic isoforms of rabbit skeletal muscle subfragment 1, S1A1, and S1A2, were equally retained under the buffer conditions used. No retention to immobilized DNase I alone was observed. Binding of S1 to immobilized actin−DNase I complex was not suppressed by simultaneous inclusion of bovine serum albumin (data not shown). The adsorption of S1 to immobilized actin−DNase I complex was found to be sensitive to ionic strength; addition of 30 mM KCl led to its almost complete elution (not shown). These data are in agreement with previous reports demonstrating ATP sensitive binding of subfragment 1 to directly immobilized G-actin to avoid its polymerization (*50*, *51*).

Direct Demonstration of the DNase I−acto−S1 Complex. Sucrose density centrifugation (10−40% sucrose gradient) was used to demonstrate formation of a ternary DNase I−acto−S1 complex (see Materials and Methods for details). Figure 2A shows the protein distribution within the collected fractions of 1 mL as determined by the Bradford procedure (*42*). After addition of S1A1 to actin−DNase I complex, a single protein peak was obtained exhibiting a considerable shift toward the bottom of the gradient running at about 35% sucrose. Both S1A1 and actin−DNase I on their own migrated to much lower densities (Figure 2A). When the fractions from a run including actin−DNase I complex and S1A1 were analyzed by SDS−PAGE (Figure 2B), the simultaneous presence of DNase I, actin, and S1A1 in the peak fractions was observed, giving clear evidence for the formation of a ternary DNase I−acto−S1 complex.

Fluorescence Titration to Quantify the Interaction of S1A1 with F-, G-Actin, and Actin−DNase I. These data were extended and quantified by titration of the fluorescence of

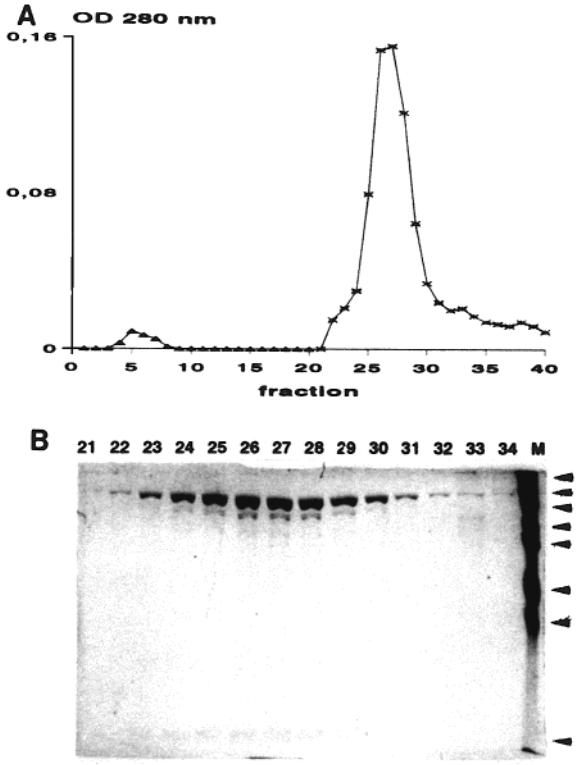

FIGURE 1: Retention of subfragment 1 (S1A1) on immobilized actin−DNase I complex. S1A1 (1 mg) in Tris-buffer (2 mM Tris-HCl, pH 8.0, 0.1 mM $CaCl_2$, 0.5 mM NaN_3) was loaded on a Mini-leak column containing immobilized actin−DNase I complex (for details see Materials and Methods). Fractions of 1 mL were collected. After tube 20, the column was washed with Tris-buffer supplemented with 2 mM ATP. (A) Optical density (OD) at 280 nm of fractions collected and (B) SDS−PAGE (10% acrylamide) of fractions 21−34. Arrowheads indicate positions of marker proteins (prestained) from top to bottom: α_2-macroglobulin (180 kDa); β-galactosidase (116 kDa); fructose-6-phosphate kinase (84 kDa); pyruvate kinase (58 kDa); fumarase (48.5 kDa); lactic dehydrogenase (36.5 kDa); triosephosphate isomerase (26.5 kDa). The lowest arrowhead indicates position of the A1 light chain.

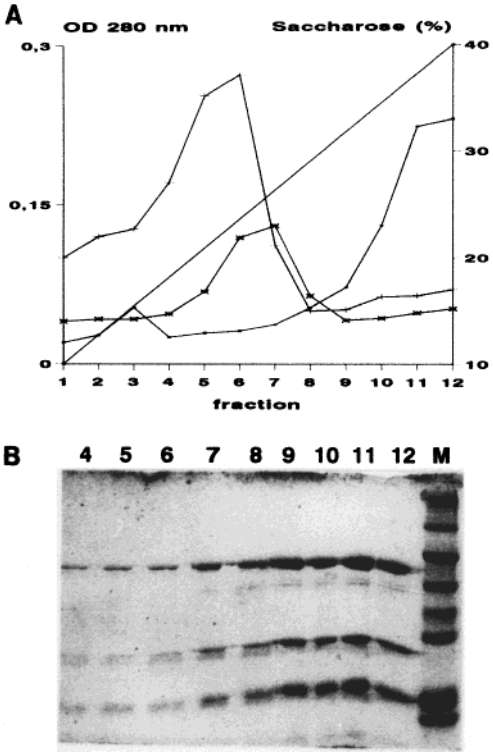

FIGURE 2: Sucrose density cosedimentation of S1 with actin−DNase I complex. Actin−DNase I complex in Tris-buffer was gel-filtered over Sephadex G-100 to remove free ATP prior to incubation with equimolar S1A1 for 15 min at RT. Then 2 mg of protein were loaded on a sucrose gradient ranging from 0 to 40%: actin−DNase I (+) or S1 on its own (*) or S1 incubated with actin−DNase I complex (■). Centrifugation and subsequent analysis was performed as detailed in Materials and Methods. Fractions of 1 mL were collected and analyzed for OD 280 (A). The fractions collected after centrifugation of the incubation mixture containing actin−DNase I complex and S1A1 were also analyzed by SDS−PAGE using a 10% acrylamide gel (B).

pyrene-labeled actin with subfragment 1. Binding of S1 to pyrenyl-G-actin results in a fluorescence increase but in a fluorescence decrease when binding to F-actin containing pyrenyl-actin. The K_D of S1A1 binding to pyrenyl-F-actin was determined by using the stopped-flow setup described previously (*48*) and resulted in a K_D of 0.54−0.96 nM in good agreement with published data (*48*).

We also used ADP-ribosylated pyrenyl-actin, which has been reported not to be able to polymerize in the presence of high salt (*40*). However, it was found that S1 induced its polymerization after an incubation period of several hours (*44*). Employing the stopped-flow procedure, we obtained a K_D of 40 nM for S1 binding to ADP-ribosylated pyrenyl-actin (not shown). This K_D value was in good agreement to measurements obtained by equilibrium titration of ADP-ribosylated pyrenyl-actin with S1A1 (*44*) and of pyrenyl-G-actin for which a K_D of about 40 nM was determined under otherwise identical conditions (Figure 3). Therefore, the experiments to be described were performed by equilibrium titration. When using pyrenyl-actin−DNase I complex a K_D of 40 nM was obtained for S1A1 binding (Figure 3). In a parallel experiment, we analyzed the DNA-degrading activity of an identical incubation mixture of pyrenyl-actin−DNase I complex with S1A1. Figure 3b demonstrates that during a period of 3 h the DNase I activity remained unchanged, i.e., inhibited, indicating that subfragment 1 binding did not induce dissociation of the actin−DNase I complex.

Chemical Cross-Linking of Subfragment 1 to Actin in Complex with DNase I. Using EDC, it was possible to chemically cross-link S1A1 to actin complexed to DNase I. A major band of Mr of 165 kDa became visible after SDS−PAGE (Figure 4a). The cross-linked material remained in the supernatant after 1 h of centrifugation at 100000*g* (Figure 4a), demonstrating that the cross-linking reaction did not induce filament formation. No cross-linking was observed when the reaction was performed in the presence of 2 mM ATP (not shown). To verify cross-linking of actin in complex with DNase I to S1, we performed immunoblots using anti-actin and -subfragment 1 antibodies. The data obtained demonstrated the presence of a new strong actin- and S1-immunoreactive band of about 165 kDa (Figure 4b). Furthermore, we observed additional immunoreactive bands: (i) a band of about 120 kDa only reactive to anti-S1 most likely representing a cross-linking product of the heavy and A1 light chains and (ii) one of about 180 kDa probably representing a cross-linking product of actin to the 120 kDa S1-A1 adduct (Figure 4b). Alternatively, actin-S1 cross-linking products involving different site chains could have been generated exhibiting different mobilities after SDS−PAGE (reviewed in ref *52*).

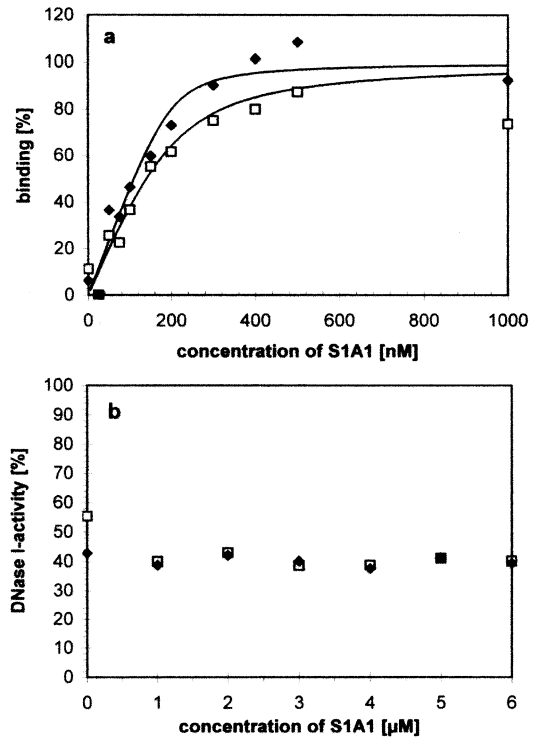

FIGURE 3: Titration of pyrenyl-G-actin and -actin−DNase I complex with S1A1. (a) Pyrenyl-G-actin (◆, 200 nM) and pyrenyl-G-actin−DNase I complex (□, 200 nM pyrenyl-G-actin, 300 nM DNase I) were incubated with increasing concentrations of S1A1. The fluorescence was measured immediately after preparing the samples. The data fitted binding curves giving K_D values of 10 nM for pyrenyl-G-actin−S1A1 complex and 40 nM for pyrenyl-G-actin−DNase I−S1A1 complex. (b) Measurement of DNase I inhibition after incubation with S1A1. G-actin−DNase I-complex (3 μM) was incubated with increasing concentrations of S1A1. The DNase I activity was measured after 1 min (□) and 3 h (◆). The DNase I-activity in absence of G-actin was set to 100%.

Fluorescence Titration of Pyrenyl-G-Actin Complexed to Other Sequestering Proteins. We also complexed pyrenyl-actin to G1, thymosin β_4, or DBP to analyze the capacity of these complexes to interact with S1A1. A fluorescence increase was only observed when titrating pyrenyl-actin in complex with Tβ_4, not when in complex with G1 or DBP (Figure 5). Since the lack of a fluorescence increase does not necessarily exclude binding of S1 to these complexes, we tested the interaction of native actin−G1 complex with S1 by competition experiments.

Fluorescence Competition Experiments of Monomeric Actins with S1 Bound to Pyrenyl-F-Actin. Binding of S1 to F-actin containing pyrenyl-labeled monomers results in a fluorescence decrease. Competition experiments were performed in which unlabeled actin competed with pyrenyl-F-actin for S1 binding (*48*). To this end, pyrenyl-F-actin stabilized by phalloidin and decorated by S1A1 was treated with increasing concentrations of native F-, G-actin, or actin complexed to DNase I or G1. A clear competition was obtained for native F-actin, G-actin, and the actin−DNase I complex (Figure 6). From the plots of fluorescence increase versus F-actin, G-actin, and actin−DNase I concentrations, the K_D values were estimated by best-fit analysis to be 0.5, 10, and 40 nM, respectively. Similarly, competition of actin−G1 complex for S1A1 with F-actin was observed, suggesting that S1A1 is also able to bind to G-actin when complexed to G1. We did not test S1 binding to actin−DBP complex

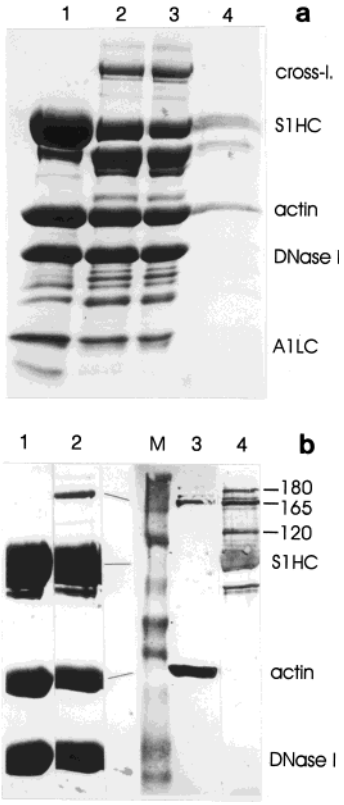

FIGURE 4: Chemical cross-linking of S1A1 to F-actin or G-actin in complex with DNase I. (a) G-actin at 11.1 μM, 22.2 μM DNase I, and 11.1 μM S1A1 in 55 mM MES-buffer, pH 6.0, were cross-linked by the addition of 0.55 mM EDC. Lane 1: 30 μL sample before cross-linking; lane 2: 30 μL sample after cross-linking and before ultracentrifugation; lane 3: 30 μL supernatant after ultracentrifugation; and lane 4: 30 μL of pellet after ultracentrifugation. (b) Immunoblots of cross-linking actin of actin−DNase I complex to S1A1. Lanes 1 and 2: Coomassie blue-stained 10% acrylamide gel after SDS−PAGE of an incubation mixture of S1A1 and actin−DNase I at identical concentrations as in panel (a) before and after chemical cross-linking with 0.55 mM EDC, respectively. Lanes 3 and 4: Western blot of similar gels stained with monoclonal anti-actin and polyclonal anti-S1, respectively. M gives prestained marker proteins transferred to nitrocellulose as in Figure 1. Numbers on margins give estimated molecular mass (kDa) of the cross-linked products.

using this assay. Since DBP competes with G1 but not with DNase I for actin binding (*53*), the DBP binding interface on actin was assumed to be similar to that of G1. Indeed, the recent structure analyses of actin−DBP complex demonstrated that most of subdomain 1 of actin is not covered by DBP (*20*, *21*).

Alteration in the Pattern of S1-Trypsineolysis by Actin−DNase I Complex. A traditional method to probe the binding of actin to S1 is the analysis of the tryptic cleavage pattern of S1 (*5*). Trypsin cleaves the heavy chain (HC) of S1 into three defined fragments of Mr of 25 kDa (N-terminal), 50 kDa, and 20 kDa (C-terminal). In the presence of F-actin, the cleavage at the 50 to 20 kDa junctional region is protected, whereas internally cross-linked G-actin has been shown to protect the 25−50 kDa junction (*26*, *27*, *54*). We analyzed the time-dependent changes of the trypsin cleavage pattern of S1A1 after preincubation with F-actin, actin−DNase I, actin−G1, and actin−DBP complex in the absence of free ATP. In the absence of actin, the S1HC was cleaved already after 10 min into the identifiable fragments of 75, 70, 50, 25, and 20 kDa, and furthermore the A1 light chain

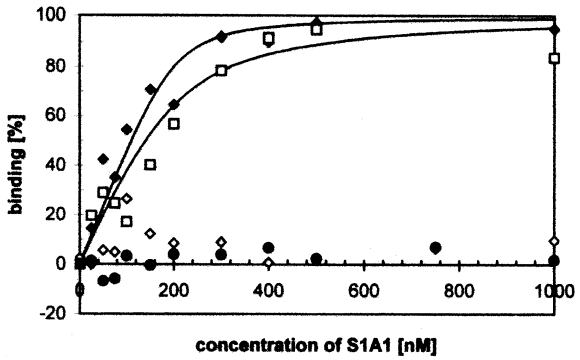

FIGURE 5: Titration of pyrenyl-actin with S1A1. Free pyrenyl-G-actin (◆, 200 nM) and preformed pyrenyl-G-actin (200 nM) in complex with an actin binding protein (300 nM) were incubated with increasing concentrations of S1A1. Immediately after preparing the samples the fluorescence was read. The symbols correspond to the following G-actin complexes: pyrenyl-G-actin−DbP complex (◇), pyrenyl-G-actin−Tβ_4 complex (□) and pyrenyl-G-actin−G1 complex (●). The solid lines represent calculated binding curves with K_D values of 10 and 40 nM.

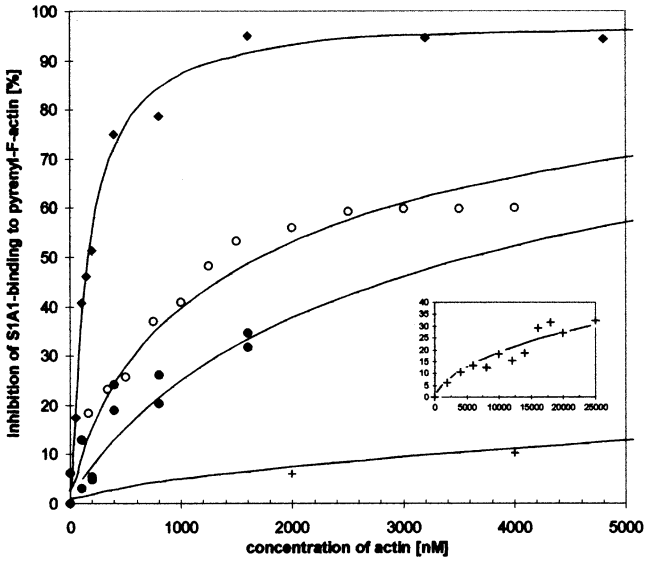

FIGURE 6: Fluorescence titration competition experiments. **(◆)** Competition with unlabeled F-actin (positive control). The protein concentrations used in this assay were 120 nM filamentous pyrenyl-actin/190 nM phalloidin, 145 nM S1A1 and increasing amounts of unlabeled F-actin. A K_D value of 0.5 nM for S1A1-binding to unlabeled F-actin was determined. The K_D value of 0.5 nM for S1A1 binding to pyrenyl-F-actin was obtained by stopped-flow measurements (data not shown). **(○)** Competition with unlabeled G-actin. The final protein concentrations were 120 nM filamentous pyrenyl-actin/190 nM phalloidin, 134 nM S1A1 and increasing amounts of G-actin. From calculated theoretical binding curves a dissociation constant of 10 nM was determined. (●) Competition with unlabeled G-actin−DNase I-complex. The final protein concentrations were 30 nM filamentous pyrenyl-actin/45 nM phalloidin, 60 nM S1A1 and increasing concentrations of unlabeled actin−DNase I complex. To determine the K_D value actin−DNase I complex concentrations of maximal 1600 nM were considered. At higher complex concentrations small amounts of free DNase I induces the depolymerization of pyrenyl-F-actin/phalloidin. The calculated K_D value was determined to be about 40 nM. In this experiment different sample preparations were used to obtain more reliable results. (+) Competition with unlabeled G-actin−gelsolin−segment 1 complex. The protein concentrations in this assay were 120 nM filamentous pyrenyl-actin/230 nM phalloidin, 160 nM S1A1 and increasing amounts of unlabeled G-actin−gelsolin segment 1 (G1) complex as given in the inset. The K_D value was determined to be about 550 nM.

was found to be hydrolyzed (Figure 7b). In the presence of F-actin, the predominantly generated fragments were of 70 and 25 kDa, but very little 50 and 20 kDa fragments (Figure 7). A similar pattern was obtained in the presence of 2.5-fold molar excess of actin−G1 complex (Figure 7b,c). A mixed pattern was observed for actin in complex with DNase I or DBP. In the presence of 2.5-fold molar excess of these complexes, the fragments 75, 70, 50, 25, and 20 kDa were generated, although with a tendency to protect the 50 to 20 kDa junction, since the 70 kDa band appeared to be stronger than for S1A1 on its own (Figure 7b,c). In the presence of actin−DBP, the 75 kDa fragment appeared to accumulate, suggesting that this complex protected both junctional regions of subfragment 1 as observed for high concentrations of chemically modified G-actin (*54*). However, when actin−DNase I complex was added at equimolar ratio to S1 preferential protection of the 25−50 kDa junction was obtained in agreement with (*54*, not shown). In contrast, after inclusion of 2 mM ATP into the incubation mixture of all complexes the cleavage pattern of the S1HC was identical to S1 in the absence of actin (not shown). The data seem to suggest that the mode of interaction of S1A1 with actin−G1 was most similar to F-actin. However, the observed degradation of G1 might have led to a loss of its polymerization inhibitory capacity. The mixed cleavage pattern in the presence of actin complexed to DNase I or DBP may have been caused by the inclusion of 1 mM $MgCl_2$ (see below) or indicate that the interaction of these complexes with subfragment 1 does not completely resemble that of F-actin.

Analysis of the Effect of Actin−DNase I Complex on the Mg^{2+}-Dependent S1-ATPase. The Mg^{2+}-dependent ATPase activity of S1 is dramatically stimulated by addition of F-actin. Previous reports have indicated that G-actin has no stimulatory effect on the S1-ATPase (*55*), although these experiments were hampered by the fact that the necessary inclusion of Mg^{2+}-ions will eventually lead to actin polymerization. However, these data were supported by results obtained with chemically modified monomeric actin (*26*, *27*) also showing a lack of S1-ATPase stimulation with the exception of G-actin after introducing an intramolecular cross-link between Cys10 and Cys374 which was able to stimulate the S1-ATPase almost like F-actin (*28*). We tested the effect of increasing concentrations of actin−DNase I complex on the Mg^{2+}-dependent ATPase of 20 μg of S1A1, but did not detect a significant stimulation at low ionic strength: 200 μg of actin−DNase I complex resulted in a 2-fold increase of the ATPase activity at 0.5 mM $MgCl_2$ (not shown, but see ref *12*). Under identical conditions, 200 μg of F-actin stimulated the S1A1-ATPase 12-fold. However, the reduced stimulatory effect of actin−DNase I might also be due to the observed decrease of S1A1 affinity to actin−DNase I complex in the presence of Mg^{2+} ions (see also Figure 9).

Interaction of Dictyostelium S1s with G-Actin. We also tested the binding of wild-type and a mutant of subfragment 1 of Dictyostelium myosin II to actin−DNase I and F-actin. The Dicty-S1-mutant 12/20-Q532E contains six additional lysine residues within a 20 residues long insertion into loop 2 and an Q532E exchange within the hydrophobic helix−turn−helix motif (*32*). This mutant S1 was constructed with the assumption that additional positive charges within the

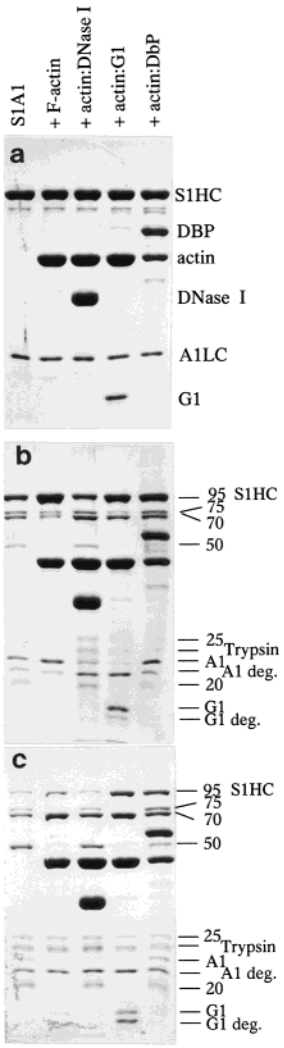

FIGURE 7: Proteolytic cleavage of S1A1 incubated with F-actin and G-actin in complex with DNase I, G1, or DBP. S1A1 at 4 μM was preincubated for 2 h on its own, with 10 μM F-actin or G-actin in complex with DNase I, G1, or DBP in 5 mM Hepes-OH, pH 7.4, 1 mM $MgCl_2$, 0.1 mM $CaCl_2$, and 0.5 mM NaN_3. Before polymerization and formation of the G-actin complexes, the actin was treated with Dowex 1X8 for 1 min to remove free ATP. Thereafter trypsin at 1/100 weight ratio to actin was added and the mixture was further incubated at room temperature. Aliquots for SDS−PAGE were collected before addition of trypsin (a) or 10 min (b) and 30 min (c) after addition of trypsin. SDS−PAGE was performed on 12% polyacrylamide gels.

actin binding loop 2 should increase its affinity to F-actin which has been shown to be indeed the case (*31*, *32*). Titration of pyrene-labeled actin−DNase I complex with wild-type dictyostelium S1 showed a K_D of 15 μM being much higher than for skeletal S1A1, which has been attributed to the fact that residue 532 of skeletal muscle S1 is glutamate (E) instead of glutamine (Q). The affinity of the 12/20-Q532E mutant to actin−DNase I was higher: we determined a K_D of 400 nM (Figure 8) being still of lower affinity than skeletal muscle S1A1 (K_D = 100 nM) under identical conditions.

Dependence on Ionic Strength of the Interaction of S1 with Monomeric Actins. Binding of S1 to F-actin is believed to occur in discrete steps starting from a low affinity collision complex governed by electrostatic interactions (weak binding) to a high affinity stereospecific complex stabilized by both hydrophobic and ionic interactions (*2*−*4*, *56*). To

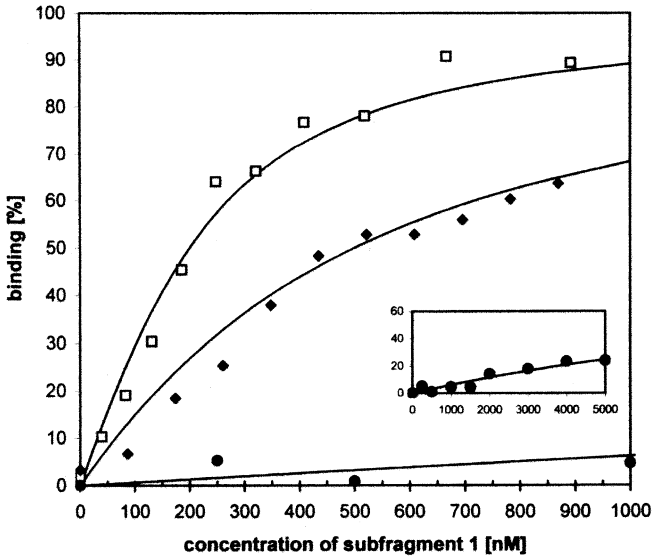

FIGURE 8: Titration of pyrenyl-actin−DNase I with Dictyostelium S1s. Pyrenyl-G-actin−DNase I-complex (200 nM pyrenyl-G-actin, 300 nM DNase I) was incubated with increasing concentrations of skeletal muscle S1A1 (□), Dictyostelium S1 (K12/20-Q532E) mutant (◆), and wild-type Dictyostelium S1 (●). The solid lines correspond to theoretical binding curves calculated with K_D values of 100 nM, 400 nM, and 15 μM, respectively.

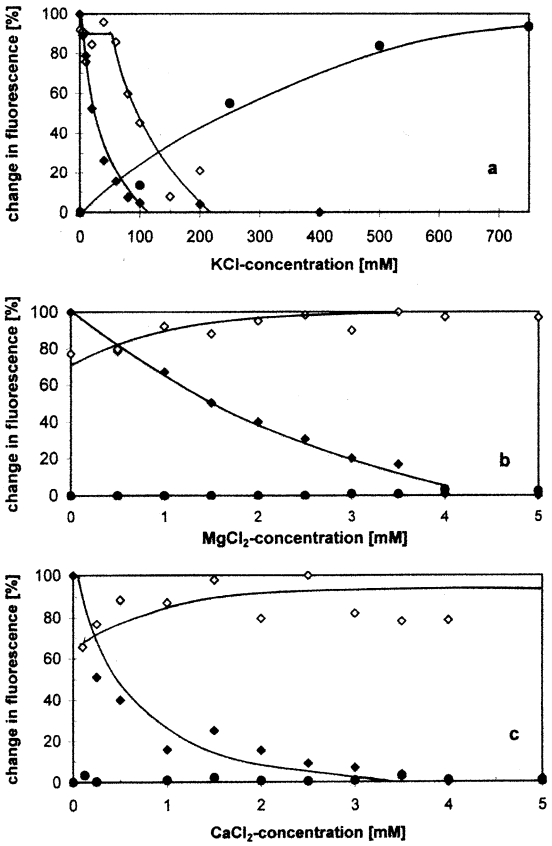

FIGURE 9: Ionic dependence of the interaction of S1s with F-actin or actin−DNase I complex. 400 nM pyrenyl-G-actin−DNase I−S1A1 complex (◆), 400 nM pyrenyl-F-actin/phalloidin decorated with S1A1 (●) or 200 nM pyrenyl-G-actin−DNase I−S1−K12/20-Q532E mutant (◇) were treated with increasing concentrations of KCl (a), $MgCl_2$ (b), and $CaCl_2$ (c). The range of the maximal fluorescence change was determined in the absence or presence of 1 mM ATP and set to 100%.

identify the mode of interaction of S1 with monomeric actin, we first analyzed the ionic dependence of skeletal S1 binding

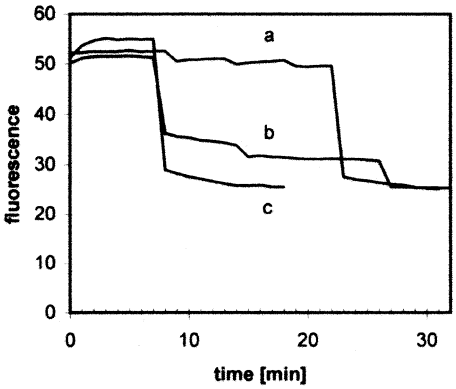

FIGURE 10: Displacement of mant-ADP from S1A1 by F-actin or actin−DNase I complex. S1A1 (1 μM) was pretreated with 0.5 μM mant-ATP. After an incubation period of 20 min, the kinetic assay was started by stepwise addition of 1 μL of (a) buffer alone, (b) actin−DNase I complex resulting in increments of 2 μM G-actin in complex with 2.5 μM DNase I (final concentration), or (c) F-actin (increments of 2 μM final concentration). Both actins were employed immediately after their pretreatment with Dowex 1X8 to remove excess unlabeled ATP. ATP to a final concentration of 1 mM was added at the end of the assay to estimate the amount of mant-ADP that had not been displaced. (a) Addition of buffer after 8, 13, and 18 min and ATP after 22 min. (b) Addition of actin−DNase I complex after 7, 14, and 20 min and ATP after 26 min. (c) Addition of F-actin after 7 and 14 min.

to pyrenyl-actin−DNase I complex. As can be seen from Figure 9a, an increase in KCl concentration significantly reduced the binding of S1A1 to pyrenyl-actin−DNase I complex. At 50 mM KCl, an almost complete decrease of the specific fluorescence signal was obtained. Addition of increasing $CaCl_2$ or $MgCl_2$ concentrations also induced dissociation of this complex being almost complete at 5 mM (Figure 9b,c), in agreement to the results obtained by using the actin−DNase I affinity column.

Due to the low affinity of dictyostelium wt S1 to actin−DNase I complex, we were not able to measure the salt dependence of this interaction. However, it was possible to perform these experiments for the double mutant Dictyostelium S1. It was found that the complex of 12/20-Q532E mutant and actin−DNase I complex remained stable up to 60 mM KCl, but dissociated when KCl was further increased (Figure 9a). In contrast, this complex remained stable or even increased in stability when increasing the $CaCl_2$ or $MgCl_2$ concentrations (Figure 9b,c).

Displacement of mant-ADP from S1 by Actin−DNase I Complex. Albeit spatially separated, the actin binding and ATPase center of S1 have been shown to communicate (for review see ref *24*). The transition from a weakly to strongly F-actin attached S1 is accompanied by the stimulation of the product release steps from the nucleotide binding site (see ref *24*). We therefore asked whether binding of S1 charged with ADP to actin−DNase I complex would stimulate ADP release. To this end, we preincubated rabbit skeletal S1 with a substoichiometric amount of the fluorescent ATP analogue mant-ATP for 30 min. Release of generated mant-ADP was determined by the decrease in the mant-fluorescence after addition of actin−DNase I complex or F-actin (Figure 10). A slightly lower decrease in mant-fluorescence than after addition of F-actin was obtained for actin−DNase I complex; however, the kinetics of the release steps were not further analyzed.

DISCUSSION

The interaction of skeletal muscle myosin with F-actin leads to the formation of force generating cross-bridges and stimulation of the Mg^{2+}-dependent myosin ATPase. Each of the two globular heads of myosin possesses one actin binding site and one ATPase center that are located on the N-terminal motor domain of subfragment 1. In contrast, the interaction of the motor domain with G-actin has been regarded as either nonexistent or nonphysiological. However, a number of previous reports have indicated an interaction of S1 with monomeric actin (*7*−*10*). In this report, we extend these observations and present evidence for a specific interaction of S1 with monomeric actin bound to different sequestering proteins.

Our data demonstrate that S1 is able to interact with actin complexed to the binding proteins employed, although with an affinity up to 100-fold lower than to F-actin. Using fluorescence techniques, we did not observe marked differences in the dissociation constants of S1 from actin complexed to DNase I or thymosin β_4, although these proteins are known to bind to different regions on actin. It was only possible to determine binding of S1 to the actin−G1 complex by the competition procedure and inferred from the proteolytic cleavage pattern. Similar to the interaction of S1 with F-actin, binding of S1 to monomeric actin was ATP sensitive, demonstrating that the affinity of S1 to G-actin is also influenced by the occupancy of the nucleotide binding pocket of S1 and furthermore suggesting that identical regions of the S1 molecule are involved in this interaction. The high sensitivity of the S1 binding to monomeric actin on salt concentration suggests that this interaction is predominantly ionic. It may therefore resemble the initial step of S1 attachment to F-actin. We assume, however, that the determined K_D of about 50 nM is too low for representing only a primary collision complex.

The main contact of DNase I to actin is on a loop comprising residues 42−48 of subdomain 2 (*17*), whereas G1 binds between subdomains 1 and 3 of actin (*18*). In contrast, thymosin β_4 is thought to span the region between the G1 and DNase I binding sites (*19*). However, all these actin binding proteins do not cover the surface of subdomain 1 which from image reconstruction data of EM pictures of fully decorated F-actin was shown to represent the main binding region for S1 on actin (*2*, *3*, *25*).

The structure of subfragment 1 has often been compared with a tadpole where the head corresponds to the bulk of the molecule containing the actin binding site at its tip and at a distance of 4 nm the ATPase center on its back. The tail of the tadpole corresponds to the α-helical lever arm. The atomic structure of a number of S1 molecules (from chicken skeletal muscle and Dictyostelium) has been fitted into EM image reconstruction data of the appropriate fully decorated F-actin. These analyses have suggested that actin binding is mediated by at least four different structural elements of S1. The so-called loop 2 (residues 626−647 in chicken skeletal S1) connecting the lower part of the 50 kDa to the C-terminal 20 kDa fragment is supposed to bind to the negatively charged N-terminus of actin (residues 1−4 and 23 and 24) and to be primarily responsible for the initial ionic contact. An additional loop originating from the tip of the upper 50 kDa fragment, the so-called cardiomyopathy

loop (residues Pro404 to Lys415), was demonstrated to bind to Pro332 and Glu334 of actin. Furthermore, underneath the lower 50 kDa fragment of S1 there exists a hydrophobic site (helix−turn−helix motif, Pro529 to His558) which is thought to bind to a hydrophobic patch at the lower part of subdomain 1 at the region of the C-terminus of actin (for reviews see refs *4* and *24*). It is assumed that these contact areas are established between S1 and a single actin monomer. We assume that S1 binding to actin−DNase I complex occurs via these contacts, since they are not covered by DNase I. In contrast, the C-terminal hydrophobic patch of actin comprising residue Ala144 and the helix from residue 340 to Leu349 containing a number of solvent-exposed hydrophobic residues will be covered by G1 (*18*) and by DBP (*20*, *21*). Indeed, we observed a lower affinity of S1 to actin−G1 complex. In addition, a secondary actin binding site at the lower 50 kDa fragment has been recognized which binds to subdomain 2 of the next actin monomer down the long pitch helix (possibly Glu93; *4*). This contact will not be established when S1 binds to monomeric actin. However, it has been reported that S1 can bind to or induce the formation of actin dimers when interacting with chemically modified monomeric actin (*54*, *57*). We are however confident that employing actin in complex with sequestering proteins excluded actin dimerization, since no indication for a dimerization process was obtained from our fluorescence measurements. Furthermore, a previous report using chemically cross-linked G-actin−S1 in complex with DNase I excluded actin dimerization (*58*).

It has been shown that loop 2 is protected from proteolytic cleavage when bound to F-actin (*5*). Indeed, we obtained protection of the 50−20 kDa junction of S1 in the presence of actin in complex with DNase I, G1, or DBP indicating interaction of the charged N-terminus of complexed actin with S1. The high ionic sensitivity of this interaction suggests that this contact region probably together with the cardiomyopathy loop predominates in the interaction of S1 with monomeric actins. Further evidence of this assumption was provided by the stronger binding of the Dictyostelium S1 mutant containing an increased number of positively charged residues within loop 2 than wild-type Dictyostelium S1. Their binding was also stable at increased ionic strength, possibly suggesting a contribution of hydrophobic interactions.

The interaction of myosin and F-actin is believed to occur in three steps (*4*): an (i) initial collision complex dominated by weak electrostatic interactions leads to the formation of (ii) an attached state of low-affinity (A-state). The A-state is transformed into an attached state of high-affinity (R-state). The equilibrium between A- and R-state is determined by the nucleotide bound to S1, the R-state being strongly favored by the product (P_i and ADP) release steps stimulated by actin. The R-state is supposed to be identical to the rigor state characterized by high affinity binding of nucleotide-free S1 to F-actin. All image reconstructions of the acto-S1 complex have been performed with this complex.

We determined binding of S1 to monomeric actins in the absence of nucleotide. The affinity determined for this interaction was about 50−100-fold lower than to F-actin. We therefore suppose that the R-state is not attained when S1 binds to monomeric actin, also because the S1-ATPase is only weakly increased by the actin−DNase I complex. Nevertheless, we assume that the interaction of S1 with monomeric actin might recapitulate the initial steps of the interaction of S1 with actin during active cycling and resemble more closely the A-state, although under nucleotide-free conditions. We hope that complexes of S1 with monomeric actin will become amenable to structural studies.

ACKNOWLEDGMENT

It is a pleasure for us to acknowledge the technical assistance of Mrs. U. Ritenberg and to thank Profs. M. Geeves and R. S. Goody (Max-Planck-Institute of Molecular Physiology, Dortmund, Germany) for help with the initial stopped-flow measurements.

REFERENCES

1. Straub, F. B. (1942) *Actin*. In *Studies from the Institute of Medical Biochemistry, University of Szeged*, Vol. 3, pp 23−37, Szeged, Hungary.
2. Rayment, I., Holden, H. M., Whittaker, M., Yohn, C. B., Lorenz, M., Holmes, K. C., and Milligan, R. A. (1993) *Science 261*, 58−65.
3. Schröder, R. R., Manstein, D. J., Jahn, W., Holden, H., Rayment, I., Holmes, K. C., and Spudich, J. A. (1993) *Nature 364*, 171−174.
4. Volkmann, N., and Hanein, D. (2000) *Curr. Opin. Cell Biol. 12*, 26−34.
5. Mornet, D., Bertrand, R., Pantel, P., Audemard, E., and Kassab, R. (1981) *Nature 292*, 301−306.
6. Amos, L. A., Huxley, H. E., Holmes, K. C., Goody, R. S., and Taylor, K. A. (1982) *Nature 299*, 467−469.
7. Chaussepied, P., and Kasprzak, A. A. (1989) *Nature 342*, 950−953.
8. DasGupta, G., White, J., Cheung, P., and Reisler, E. (1990) *Biochemistry 29*, 8503−8508.
9. Chen, T., and Reisler, E. (1991) *Biochemistry 30*, 4546−4552.
10. Schick, B., Kiessling, P., Polzar, B., and Mannherz, H. G. (1993) *Eur. J. Cell Biol. 62*, 205−213.
11. Lazarides, E., and Lindberg, U. (1974) *Proc. Natl. Acad. Sci. U.S.A. 71*, 4742−4746.
12. Mannherz, H. G., Barrington Leigh, J., Leberman, R., and Pfrang, H. (1975) *FEBS Lett. 60*, 34−38.
13. Hitchcock, S. E., Carlsson, L., and Lindberg, U. (1976) *Cell 7*, 531−543.
14. Van Baelen, H., Bouillon, R., and DeMoor, P. (1980) *J. Biol. Chem. 255*, 2270−2272.
15. Way, M., Gooch, J., Pope, B., and Weeds, A. G. (1989) *J. Cell Biol. 109*, 593−605.
16. Safer, D., Golla, R., and Nachmias, V. T. (1990) *Proc. Natl. Acad. Sci. U.S.A. 87*, 235−238.
17. Kabsch, W., Mannherz, H. G., Pai, E., Suck, D., and Holmes. K. C. (1990) *Nature 347*, 37−44.
18. McLaughlin, P. J., Gooch, J., Mannherz, H. G., and Weeds, A. G. (1993) *Nature 364*, 685−692.
19. Ballweber, E., Hannappel, E., Huff, T., Stephan, H., Haener, M., Taschner, N., Stoffler, D., Aebi, U., and Mannherz, H. G. (2002) *J. Mol. Biol. 315*, 613−625.
20. Otterbein, L. R., Cosio, C., Graceffa, P., and Dominguez, R. (2002) *Proc. Natl. Acad. Sci. U.S.A. 99*, 8003−8008.
21. Head, J. F., Swamy, N., and Ray, R. (2002) *Biochemistry 41*, 9015−9020.
22. Sutoh, K. (1982) *Biochemistry 21*, 3654−3661.
23. Bertrand, R., Chaussepied, P., and Benyamin, Y. (1988) *Biochemistry 27*, 5728−5736.
24. Geeves, M. A., and Holmes, K. C. (1999) *Annu. Rev. Biochem. 68*, 687−728.
25. Milligan, R. A. (1996) *Proc. Natl. Acad. Sci. U.S.A. 93*, 21−26.
26. Bettache, N., Bertrand, R., and Kassab, R. (1989) *Proc. Natl. Acad. Sci. U.S.A. 86*, 6028−6032.
27. Bettache, N., Bertrand, R., and Kassab, R. (1990) *Biochemistry 29*, 9085−9091.
28. Heintz, D., and Faulstich, H. (1996) *Biochemistry 35*, 258−265.
29. Chen, T., Haigentz, M., Jr., and Reisler, E. (1992) *Biochemistry 31*, 2941−2946.
30. Lheureux, K., and Chaussepied, P. (1995) *Biochemistry 34*, 11435−11444.
31. Furch, M., Geeves, M. A., and Manstein, D. (1998) *Biochemistry 37*, 6317−6327.

32. Furch, M., Remmel, B., Geeves, M. A., and Manstein, D. J. (2000) *Biochemistry 39*, 11602−11608.
33. Carstens, M. E., and Mommaerts, W. F. H. M. (1963) *Biochemistry 2*, 28−32.
34. Spudich, J. A., and Watt, S. (1971) *J. Biol. Chem. 246*, 4866−4871.
35. Koujama, T., and Mihashi, K. (1981) *Eur. J. Biochem. 114*, 33−38.
36. Weeds, A. G., and Taylor, R. S. (1975) *Nature 257*, 54−56.
37. Mannherz, H. G., Goody, R. S., Konrad, M., and Nowak, E. (1980) *Eur. J. Biochem. 104*, 367−379.
38. Hannappel, E., Wartenberg, F., and Bustelo, X. R. (1989) *Arch. Biochem. Biophys. 273*, 396−402.
39. Buch, S., Gremm, D., Wegner, A., and Mannherz, H. G. (2002) *Biol. Chem. 383*, 1621−1631.
40. Aktories, K., Bärmann, M., Ohishi, I., Tsuyama, S., Jacobs, K. H., and Habermann, E. (1986) *Nature 322*, 390−392.
41. Lehrer, S. S., and Kerwar, G. (1972) *Biochemistry 28*, 1211−1217.
42. Bradford, M. M. (1976) *Anal. Biochem. 72*, 248−254.
43. Laemmli, U. K. (1970) *Nature 227*, 680−685.
44. Ballweber, E., Galla, M., Aktories, K., Yeoh, S., Weeds, A. G., and Mannherz, H. G. (2001) *FEBS Lett. 508*, 131−135.
45. Rickwood, D., Ed. (1989) *Centrifugation a Practical Approach*, IRL Press Oxford, Washington, DC.
46. Mannherz, H. G., Brehme, H., and Lamp, U. (1975) *Eur. J. Biochem. 60*, 109−116.
47. Kunitz, M. (1950) *J. Gen. Physiol. 33*, 349−362.
48. Kurzawa, S. E., and Geeves, M. A. (1996) *J. Muscle Res. Cell Motil. 17*, 669−676.
49. Woodward, S. K. A., Eccleston, J., and Geeves, M. A. (1991) *Biochemistry 30*, 422−430.
50. Chantler, P. D., and Gratzer W. B. (1973) *FEBS Lett. 34*, 10−14.
51. Chantler, P. D., and Gratzer W. B. (1976) *Biochemistry 18*, 2219−2225.
52. Chaussepied, P., and van Dijk, J. (2002) in *Results and Problems in Cell Differentiation: Molecular Interactions of Actin* (Thomas, D. D., and dosRemedios, C. G., Eds.) pp 51−64, Springer-Verlag, Berlin Heidelberg.
53. Ballweber, E., Hannappel, E., Huff, T., and Mannherz, H. G. (1997) *Biochem. J. 327*, 787−793.
54. Arata, T. (1996) *Biochemistry 35*, 16061−16068.
55. Offer, G., Baker, H., and Baker, L. (1972) *J. Mol. Biol. 252*, 2891−2899.
56. Geeves, M. A., and Conibear, P. B. (1995) *Biophys. J. 68*, 194S−199S.
57. Valentin-Ranc, C., Combeau, C., Carlier, M.-F., and Pantaloni, D. (1991) *J. Biol. Chem. 266*, 17872−17879.
58. Lheureux, K., and Chaussepied, P. (1995) *Biochemistry 34*, 11445−11452.

BI020597Q